Construction and Building Materials 352 (2022) 129019

Contents lists available at ScienceDirect

Construction and Building Materials

journal homepage: www.elsevier.com/locate/conbuildmat

Pre-bcc: A novel integrated machine learning framework for predicting mechanical and durability properties of blended cement concrete

Hisham Hafez [a,*], Ahmed Teirelbar [b], Rawaz Kurda [c], Nikola Tošić [d], Albert de la Fuente [d]

[a] Laboratory of Construction Materials, EPFL, CH-1015 Lausanne, Switzerland
[b] Chief Technical Officer, Digified, Cairo, Egypt
[c] CERIS, Civil Engineering, Architecture and Georesources Department, Instituto Superior Técnico, Universidade de Lisboa, Av. Rovisco Pais, 1049-001 Lisbon, Portugal
[d] Civil and Environmental Engineering Department, Universitat Politècnica de Catalunya, Jordi Girona 1–3, 08034 Barcelona, Spain

ARTICLE INFO

Keywords:
Supplementary cementitious materials
Blended cement concrete
Strength prediction
Durability prediction
Regression model

ABSTRACT

Partially replacing ordinary Portland cement (OPC) with low-carbon supplementary cementitious materials (SCMs) in blended cement concrete (BCC) is perceived as the most promising route for sustainable concrete production. Despite having a lower environmental impact, BCC could exhibit performance inferior to OPC in design-governing functional properties. Hence, concrete manufacturers and scientists have been seeking methods to predict the performance of BCC mixes in order to reduce the cost and time of experimentally testing all alternatives. Machine learning algorithms have been proven in other fields for treating large amounts of data drawing meaningful relationships between data accurately. However, the existing prediction models in the literature come short in covering a wide range of SCMs and/or functional properties. Considering this, in this study, a non-linear multi-layered machine learning regression model was created to predict the performance of a BCC mix for slump, strength, and resistance to carbonation and chloride ingress based on any of five prominent SCMs: fly ash, ground granulated blast furnace slag, silica fume, lime powder and calcined clay. A database from>150 peer-reviewed sources containing>1650 data points was created to train and test the model. The statistical performance was found to be comparable to that of existing models ($R = 0.94$–0.97). For the first time, the model, *Pre-bcc*, was also made available online for users to conduct their own prediction studies.

1. Introduction

Concrete production is one of the predominant factors contributing to the environmental impacts of the built environment [1]. Ordinary Portland cement (OPC) production is the major contributor to the environmental impact of concrete. One tonne of OPC production produces approximately 900 kg of CO_2, half of which directly results from the calcination of the raw materials [2]. Blended cement concrete (BCC) is a type of concrete where OPC is partially replaced with various pozzolanic materials called supplementary cementitious materials (SCMs). The higher the SCM dosage, the more sustainable the concrete product is expected to be comparably [3]. In today's market, cements contain, on average, around 20 % of SCMs [4]. Apart from under-researched SCMs with minimal commercial presence, such as municipal incinerated bottom ash (MIBA), bauxite residue and glass slag, the most used SCMs, which are considered in the scope of this paper, are fly ash (FA), which is a by-product of coal combustion, ground granulated blast-furnace slag (GGBS), which is a by-product of steel manufacturing, silica fume (SF), which is generated from glass manufacturing, finely ground limestone which is referred to lime powder (LP) and kaolinitic clays calcined (CC) at a temperature between 700 °C and 800 °C [5]. Table 1 provides data related with the available SCM types as well as the commercial utilization of those in concrete.

The impact of replacing OPC with SCMs on the produced concrete, as will be explained in the next section, varies widely depending on the SCM type, the dosage and the mix design [6]. Hence, optimizing the properties of a BCC utilizing one or more SCMs in an attempt to produce a sustainable concrete mix is a difficult, time-consuming and only possible on an experimental case-by-case basis. This signifies the need to predict the properties of a BCC mix and reduce the size of the designed experimental campaign. The use of machine learning regression models enables the overcoming of this challenge through its ability to treat large

* Corresponding author.
E-mail addresses: hisham.hafez@epfl.ch (H. Hafez), ateirelb@digified.io (A. Teirelbar), rawaz.kurda@tecnico.ulisboa.pt (R. Kurda), nikola.tosic@upc.edu (N. Tošić), albert.de.la.fuente@upc.edu (A. de la Fuente).

https://doi.org/10.1016/j.conbuildmat.2022.129019
Received 14 February 2022; Received in revised form 1 July 2022; Accepted 29 August 2022

Table 1
A comparison between the estimated global yearly production and use in concrete for several SCMs [7].

SCM	Estimated global production volume (Mt/year)	Estimated current use as an SCM (Mt/year)
FA	700–1000	350–400
GGBS	300–350	350–400
SF	1–3	1–2
CC	large accessible reserves	2–3
LP	large accessible reserves	250–300
MIBA	30–60	0
Bauxite residue	100–150	0
Waste glass	50–100	0

amounts of data and produce useful regressions. Hence, in this paper, a non-linear multi-layered machine learning regression model (*Pre-bcc*) was developed to predict the performance of a binary or ternary BCC mix based on any of five prominent SCMs: fly ash, ground granulated blast furnace slag, silica fume, lime powder and calcined clay. The structure of the paper is as follows: Section 2 presents a literature review on SCMs and their effects on BCC properties; Section 3 describes the *Pre-bcc* regression model; Section 4, presents and discusses the results obtained by using the model; Section 5 contains a description of the model validation process; and Section 6 concludes the paper.

2. Literature review

2.1. Characterization of SCM

In a blended cement concrete mix, cement is partially replaced with an SCM. An SCM reacts either as a hydraulic, pozzolanic or a filler material, which means that its contribution to the binding characteristics is governed by a combination of its reaction with water similar to cement, its reaction with the chemical phases resulting from cement hydration processes or as a chemical catalyst, respectively [8]. Hence, the intrinsic factors that influence the performance and the degree of reactivity of an SCM are its chemical and physical composition. As shown in the ternary graph in Fig. 1, the chemical composition of any SCM is mostly a mix of calcium, silicon, and aluminium oxides.

The reactivity of an SCM is determined through the combined effect of the percentage of soluble siliceous, aluminosiliceous or calcium aluminosiliceous contents, which is a chemical characteristic and/or the surface area which is physical. The higher both values are, the more reactive an SCM is expected to be [9]. A summary of the values of the average surface area of the five SCMs understudy is presented in Table 2.

2.2. Functional properties of BCC

2.2.1. Workability

Workability is the ease by which fresh concrete can be cast, compacted (with the means available) and finished in the formwork for the intended shape. The more workable a concrete mix is, the easier it flows, which makes self-compacting concrete (SSC) a special concrete with the highest workability, more suitable for use in heavily reinforced elements [18]. Workability could be attributed to the available free water in the concrete mix, which is dependent on the ratio between the volume of the paste and the volume of the aggregates [19]. Workability as a fresh property of concrete is universally measured using a standard slump test

Table 2
A review from the literature of the physical characteristics of the SCMs under study.

	Shape	Reference	Surface area (m^2/kg)	Reference
FA	Spherical	[10]	300–500	[15]
GGBS	Angular	[11]	350–450	[16]
SF	Spherical	[12]	10,000–20,000	[17]
LP	Angular	[13]	700–1300	[17]
CC	Angular	[14]	15,000–20,000	[9]

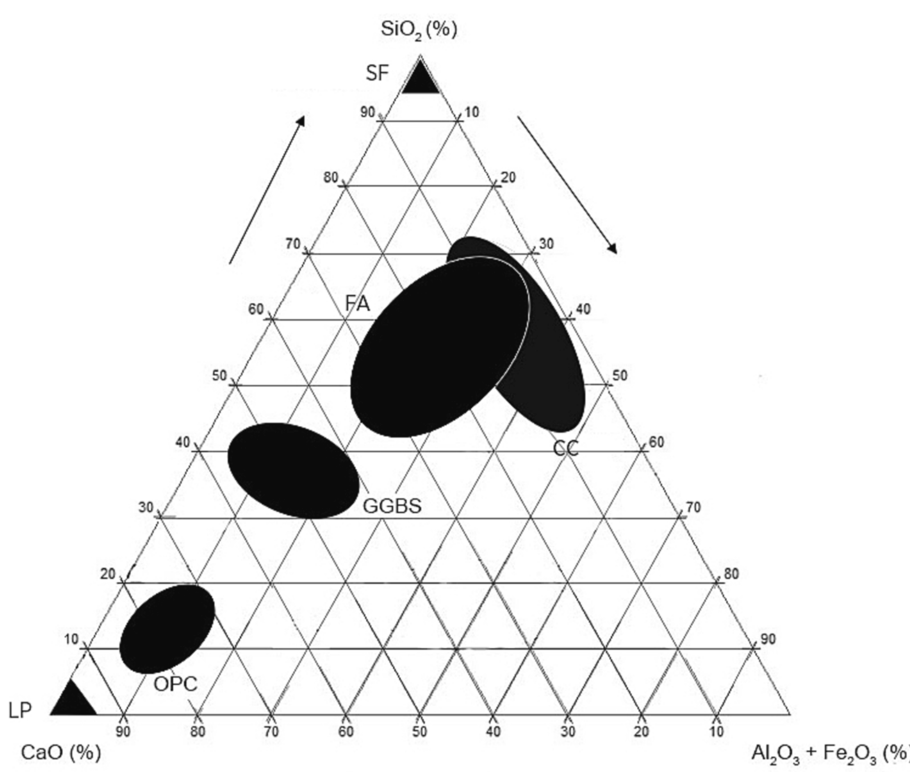

Fig. 1. A ternary diagram showing the chemical composition of OPC versus the SCMs under study.

such as ASTM C143/C143M-00 [20]. Because of the glassy structure of GGBS, the particles require less water to be coated, which causes a better slump [21]. The spherical shape of the FA particles allows it to cause a ball bearing effect reducing the water demand of the concrete mix as well [22]. Moreover, the high surface area of LP, while this being chemically inert, allows it to act well as a filler and reduce the water demand of concrete increasing the slump [17]. While replacing OPC by FA at any percentage would increase slump, it is reported to only be the case for up to 50 % GGBS and 15 % LP replacement rates. At the same time, the large surface area of both SF and CC, acts counter-effectively to increase the water demand for BCC concrete mixes and decrease their slump. The higher the replacement percentage of both SCMs for OPC, the higher the expected drop in slump is [8].

2.2.2. Compressive concrete strength

Compressive concrete strength (f_c) is the most representative indicator of the mechanical performance of a concrete mix, and other mechanical properties (i.e., tensile strength, modulus of elasticity) can be directly correlated with it for design purposes. A standard test BS EN 12390–3 to determine f_c should be carried out at 28 days [23]. The governing mix design parameter in most concrete types responsible for determining its strength is the water to binder (*w/b*) ratio [24]. Hence, the use of superplasticizers (SPs) to decrease the *w/b* ratio at a fixed slump class would increase strength [25]. However, in ultra-high strength concrete, the quality of the used aggregates become the dominant parameter [26]. The governing chemical reaction among SCMs when replacing OPC is pozzolanic [27]. The high pH level (>12) of the pore solution dissolves the inert anhydrous coating of FA and GGBS particle releasing their silicon, calcium and aluminium ions into the solution. The latter then reacts with the calcium hydroxide from the OPC hydration to form calcium silicate hydrates that occupy a larger volume and exhibit higher strength than the calcium hydroxide [28]. This latent hydraulic behaviour dictates that BCC containing FA and GGBS slow down the initial setting of OPC and hence decrease the early age strength of the binder. However, up until 30 % and 70 % replacement of OPC respectively, the strength of concrete increases marginally (<10 %) at curing age of 28 days and more at 90 days (>30 %) [29]. Although the chemical reaction by which SF and CC develop their strength-carrying calcium silicate hydrate phases is also pozzolanic, the mechanism is different than that of FA and GGBS. Owing to their extremely fine particle size, both SCMs are very reactive when replacing OPC enabling the densification and thickness reduction of the interfacial transitional zone of the binder matrix [30]. This leads to very early setting for the resulting BCC and higher early strength than for BCC with FA and GGBS. This means that BCC with SF and CC is expected to exhibit up to 40 % higher strength at both 28 and 90 days [31]. Regarding LP, the very large surface area, larger than FA and GGBS but smaller than that of SF and CC, allows for more nucleation and hydration of OPC, hence increasing the strength of the resulting BCC. However, due to the limited pozzolanic activity of LP as an SCM, its minor increase of strength (<15 %) is only limited to when it replaces 10–15 % of OPC [7].

2.2.3. Chloride ingress

Chloride penetration is the primary mechanism for the corrosion of steel reinforcement in reinforced concrete. For the corrosion to be initiated, which means the compromise of the concrete cover, a parameter called the chloride threshold must be quantified [32]. The chloride threshold potential of a concrete mix is dependent on a set of exposure conditions such as temperature, relative humidity (RH) and percentage of free chlorides as well as intrinsic variables such as the cement type and *w/b* ratio [33], which determine the chloride diffusion coefficient of the matrix. A standard test to measure the resistance of a concrete mix against chloride ingress, which is going to be the test for which the data is collected in this paper, is called the Rapid Chloride Penetration Test (RCPT) according to ASTM C1202 – 18 [34]. The addition of SCMs as a partial replacement of OPC enhances the microstructure of the binder matrix when it comes to durability against chloride penetration. In the case of LP, the reason is the filler effect which causes an increase of the effective water to cement ratio and provides a larger space for the formation of hydration products [35]. For all other SCMs, the pozzolanic reaction replaces the Portlandite with more calcium silicate hydrate phases leading to the formation of dense and less permeable microstructure. Both factors lead to less permeability, which enhances the durability of concrete to chloride ingress [36]. It is reported that SF is the SCM with the lowest permeability as it replaces more OPC, followed by CC, FA, GGBS and finally LP [37,38]. However, it is important to note that durability of reinforced concrete is not only dependant on the permeability of the matrix. It is the coupled effect of that and the chloride threshold of the binder, which is the chloride concentration at which steel reinforcement corrosion would be initiated [39]. Although replacing OPC with CC reduced the permeability of concrete significantly, the chloride threshold of BCC with CC is 0.2 % by mass of binder, whereas for OPC it is 0.4 % and for FA-based BCC 0.6 % [37].

Table 3
A review of the impact of replacing OPC with FA, GGBS, SF, LP and CC on the functional performance of concrete.

SCM	% Replacing OPC by mass	Predicted effect on the resulting BCC mix sustainability parameters compared to OPC concrete Functional performance parameter			
		Slump	28 day compressive strength	Resistance to chloride ingress	Resistance to carbonation
FA	< 30 %	+ +	/	+	–
	> 30 %	+	–	+ +	– –
GGBS	< 70 %	+	/	+	–
	< 70 %	/	–	+ +	– –
SF	< 15 %	– –	+	+	–
	> 15 %	– –	/	+ +	– –
LP	< 15 %	+	/	+	–
	> 15 %	/	–	+ +	– –
CC	< 35 %	– –	+	+	–
	> 35 %	– –	/	+ +	– –

+ + = significant increase; + = marginal increase; / = no effect; – = marginal decrease; – – = significant decrease.

2.2.4. Carbonation

Steel reinforcement embedded in reinforced concrete elements is protected by the passive cover layer with a high pH (>11). The reaction between concrete and the CO_2 from the environment to which the concrete element is exposed causes Portlandite and other calcium-containing chemical phases within concrete to react and form calcium carbonates [40]. The durability of a concrete against carbonation-induced corrosion of steel reinforcement is hence linked to the resistance of the concrete element to such carbonation process [41]. Although SCM additions to concrete yield a denser microstructure, there is unanimous agreement within the published articles that BCC has a lower resistance to carbonation compared with OPC concrete [42]. The reason is that the pozzolanic reaction consumes Portlandite in the matrix, reducing the pH and increasing the likelihood of carbonation occurrence. Hence, regardless of the type, it is expected that FA, GGBS, SF, LP and CC would, if replaced OPC in a mix, render the resulting reinforced BCC less resistant to carbonation [43]. Accordingly, the use of BCC would be of interest in applications where concrete carbonation is not critical or coupled with corrosion-resistant reinforcement such as Fibre reinforced polymer or synthetic fibres which are also gaining a lot of research attention [44–46].

2.3. Summary of BCC functional performance

A summary of the reviewed impacts of utilizing each of the five SCMs in BCC with varying percentages of OPC replacement is shown in

Table 4
A review of the number of independent and target variables from concrete prediction models found in the literature.

Author	Year	Ref	Property	variables	CEM I	SCM			CA	FA	SP	Water	Strength	%CO_2	%RH	time
						FA	GGBS	SF								
Chandawani	2014	[19]	Slump	6	√	√	–	–	√	√	√	√	–	–	–	–
Chen	2014	[53]		7	√	√	√	–	√	√	√	√	–	–	–	–
Cihan	2019	[52]		5	√	–	–	–	–	√	√	√	√	–	–	–
Hoang and Pham	2016	[51]		5	√	–	–	–	√	√	√	√	–	–	–	–
Al-Shamiri	2019	[24]	Compressive strength	6	√	√	–	–	√	√	√	√	–	–	–	–
Golafshani	2020	[50]		7	√	√	√	–	√	√	√	√	–	–	–	–
Naseri	2020	[54]		5	√	–	–	–	√	√	√	√	–	–	–	–
Yu	2018	[55]		7	√	√	√	–	√	√	√	√	–	–	–	–
Ghafoori	2013	[56]	Chloride Ingress	7	√	√	–	√	√	√	√	√	–	–	–	–
Inthata	2013	[57]		6	√	√	–	–	√	√	√	√	–	–	–	–
Mohamed	2018	[58]		8	√	√	√	√	√	√	√	√	–	–	–	–
Najimi	2019	[59]		7	√	√	–	√	√	√	√	√	–	–	–	–
Felix	2019	[60]	Carbonation	8	√	√	√	√	–	–	–	–	√	√	√	√
Kellouche	2019	[61]		6	√	√	–	–	–	–	–	√	–	√	√	√
Luo	2014	[62]		4	√	–	–	–	–	–	–	√	–	–	√	√
Taffese	2015	[63]		10	√	√	√	√	√	√	√	√	√	–	–	√

Table 3.

2.4. Prediction modelling

Whether it being a wide experimental program in a research centre or a pre-execution trial testing for a construction project, it is inefficient in terms of resources consumption and cost to do all these tests on all possible alternatives being compared [47]. While it is relatively straightforward to test slump and strength, long term durability testing is time-consuming and, frequently, incompatible with time-span of the project. Testing the durability of concrete against chloride ingress—for example—through the ponding or immersion test such as ASTM C1556 and ASTM C1543 is expensive [36]. Similarly, testing the natural carbonation for concrete samples would take months or even years depending on the mix and exposure conditions [40]. Hence, several researchers worked in recent years on developing regression models for slump, strength, chloride ingress and carbonation of concrete. The concrete industry is not swift in adopting technologies such as regression-based prediction of the concrete mix properties due to both structural safety and contractual reasons [48]. However, an increasing number of companies are using in-house datasets to train their regression models meant to partially replace the strength testing as a quality control method, but as a first screen to minimize the testing quantities [49].

Regression is a statistical method used to determine the strength and character of the relationship between one dependent variable and a series of other variables. In applications such as that of concrete properties, where the relationship is not necessarily known, it is preferred to use machine learning (ML) methods to build the regression models [24]. ML is an application of artificial intelligence (AI) that provides systems with the ability to automatically learn and improve from experience without being explicitly programmed. ML techniques have been widely used in many engineering fields due to their ability in prioritization, optimization, planning, and forecasting. Examples of such techniques that have been used for the estimation of concrete performance indicators include Artificial Neural Network (ANN), Genetic Programming (GP), Support Vector Machine (SVM) and Biogeography-Based Programming (BBP) [50].

Hoang and Pham [51] and Cihan et al. [52] both included a slump prediction model using several machine learning algorithms that consider the mass per unit volume of coarse aggregates, fine aggregates, water, superplasticizers and cement. Although the regression results showed good statistical accuracy, the models only included OPC as a binder. Chen et al. [53] and Chandawani et al. [19] included FA and GGBS to the input variables of their models and utilized parallel hypercubic gene expression and ANNs, respectively. Although this is considered an improvement respect to the two former models, it fails at including the most representative SCMs. Scarcity of models covering the utilization of more than one SCM in concrete was also detected concerning the prediction of $f_{c,28}$, resistivity to chloride penetration and

Table 5
A review of the statistical performance of the concrete performance prediction models reviewed from the literature.

Author	Property	Training points	Testing points	R	Best RMSE	unit	MAPE* (%)	Regression model
Chandawani	Slump	395	85	0.98	2.83	mm	1.38	Hybrid GA-Artificial Neural Network (ANN)
Chen		70	24	–	90		–	Parallel hyper-cubic gene expression programming (GEP)
Cihan		80	35	–	24.7		–	Decision Tree, Random Forrest, support vector machine (SVM), partial least squares, ANNs, and Fuzzy Logic
Hoang		76	19	0.97	5.4		3.68	SVM
Al-Shamiri	Compressive	246	82	0.99	1.05	MPa	1.54	Extreme learning machine, ANN
Golafshani	strength	772	258	0.97	4.96		–	ANN and Adaptive Neuro-Fuzzy Inference System (ANFIS)
Naseri		174	58	–	4.58		–	Soccer League Competition, Water Cycle Algorithm, Genetic Algorithm, SVM, ANN, and Linear Regression
Yu		1234	527	0.97	10.4		14	Cat swarm optimisation algorithm, SVM
Ghafoori	Chloride ingress	60	12	–	–	Coulomb	5.35	Comparing linear, non-linear regression with BP-ANN
Inthata		216	54	0.96	479		12.72	BP-ANN
Mohamed		50	22	0.95	–		5.61	ANN
Najimi		50	22	–	176		–	ANN based on Forward feed artificial bee colony algorithm
Felix	Carbonation	223	56	0.93	–	mm/	–	BP-ANN
Kellouche	Depth	240	60	0.98	–	$day^{0.5}$	–	BP-ANN
Luo		30	5	–	–		5.04	Particle Swarm Optimization (PSO), BP ANN
Taffese		23	10	–	0.49		–	Neural Network, Decision Tree, Bagging and Boosting ML algorithms

*MAPE (Mean Absolute Percentage Error).

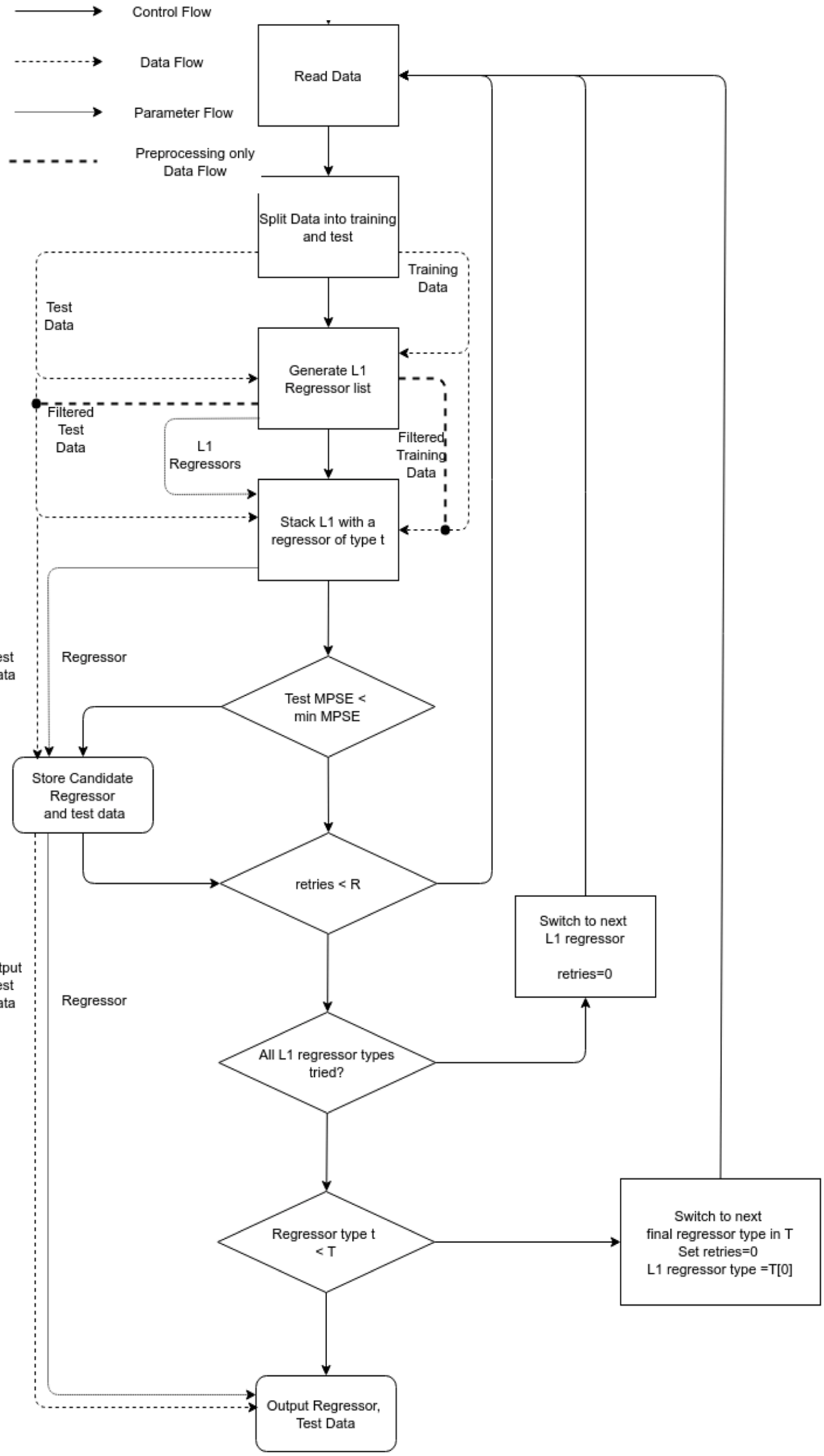

Fig. 2. A flow diagram of the pre-processing algorithm for the multi-layer regression model proposed.

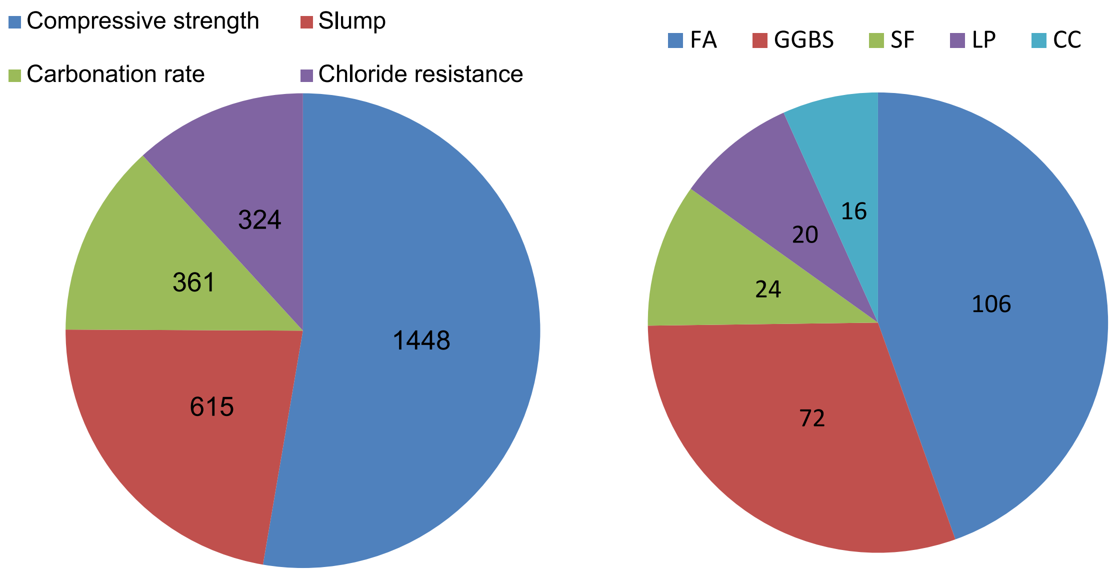

Fig. 3. The number of times each mix constituent was present in the references (left) and the number of references in each model (right) in the database developed for the *Pre-bcc* regression model generation.

natural carbonation. A summary of the input variables, type of prediction model and the number of points used to generate it from the studied literature could be found in Tables 4 and 5. The models chosen within the search scope are those correlating between these four functional parameters and BCC mixes containing one or more of the five SCMs under study.

An apparent gap found in the surveyed literature is the absence of any model that predicts the performance of lime powder or calcined clay among the rest of the SCMs. Besides, existing prediction models for chloride penetration and carbonation resulted to provide results with significant dispersion. Also, according to Kurda et al. [23], the cement grade (42.5 or 52.5) makes the fundamental difference in the strength of the resulting concrete mix in which it is used. Hence, it is also required to consider the cement grade within the parameters under study in the regression models. Finally, the sample sizes of most of the proposed models in the literature are small (<30 data points per independent variable).

3. The *Pre-bcc* regression model

Due to the complexity of the regression models under study and the objective to cover the gaps in the reviewed literature, it was decided to explore several machine learning algorithms and optimize their use according to each problem. Machine learning, as a data-driven tool, focuses on the development of computer programs that can access data and use it to auto-learn. Given a sample of observations $S = \{(\underset{-}{x},y)|\underset{-}{x} \in R^n, y \in R\}$, where $\underset{-}{x}$ is the vector of independent variables and y is the target variable, the regression problem is the search through the space of functions $(F : R^n \rightarrow R)$ for some function $f \in F$ that minimizes a defined *loss function* that describes the discrepancy between the prediction $f\left(\underset{-}{x}\right)$ and the observed value y. The *loss function* used throughout the regressors of *Pre-bcc* is the mean-squared prediction error (MSPE), Equation (1).

$$MSPE = \frac{\sum_{i=1}^{n}(EXP_i - PRE_i)^2}{n} \quad (1)$$

The search method through the function space is defined by: (1) the regression algorithm or technique and (2) the set of parameters related to the search for the learned function f not part of its definition. The targeted variables for the regressors are the concrete properties tackled within the *Pre-bcc* framework: slump, $f_{c,28}$, resistance to chloride ingress-induced corrosion through electric resistivity and natural carbonation rate. The first distinguished feature of the developed regressor is that it includes 10 independent variables: The binder content, *w/b* ratio, cement-to-binder ratio, five different types of SCMs: FA, GGBS, SF, CC and LP, coarse aggregate content-to-binder ratio, fine aggregate content-to-binder ratio, and finally, superplasticizer dosage-to-binder ratio.

3.1. Stack generation

The regression was addressed using ensemble learning methods where multiple regression learners are grouped together to provide the final prediction [64]. There are multiple ways of grouping learners to create an ensemble, the one used here is stacking or stacked generalization [65]. The first level (L1) is made up of a set of m learners $h_i : \underset{-}{x} \in R^n \rightarrow y \in R$, each of which is a result of searching a subset $S_i \subset S$ rather than the entire space. The output of these different learners is then "stacked" together along with the inputs as a vector that is fed into the second layer learner: $g : \underset{-}{z} \in R^{n+m} \rightarrow y \in R$ so that the final output of the system is $y = g(h_1(\underset{-}{x}), ..., h_m(\underset{-}{x}); \underset{-}{x})$.

There is a wide range of machine learners that could be used for boosting model, some of which were used in previous papers reviewed such as Support Vector Machine, Boot Strap Aggregations and Genetic Algorithms [19,48,55]. The learners chosen for the *Pre-bcc* regression model were the Random Forrest, Extreme Gradient (XG) Boost, Bayesian Ridge and Multi-layer Perceptron, which were implemented using off-the-shelf python codes from the scikit library [54]. After several iterations, the XGBoost model was used for all L1 learners. The final regressor is found by testing all four variants for whichever produces the lowers error.

As seen in Fig. 2, the functional database was randomly divided into 80 % training and 20 % testing groups. The training data were used to develop the model parameters, whereas the test data were used only to validate the model. Part of the challenge with this approach was how to define outliers when the underlying system being approximated is non-linear and multi-dimensional. The approach selected to identify outliers consisted in building a regression model and defining outliers as samples where the prediction error exceeds the criteria established by Naseri et al. [55]. As the L1 regressors h_i are built to each cover a subset S_i, the data $\cup_{i=0}^{m} S_i$ are maintained and if the $\left|\cup_{i=0}^{m} S_i\right| \rangle 0.8|S|$, then the model was considered a candidate and the data was saved. At the end of the pre-

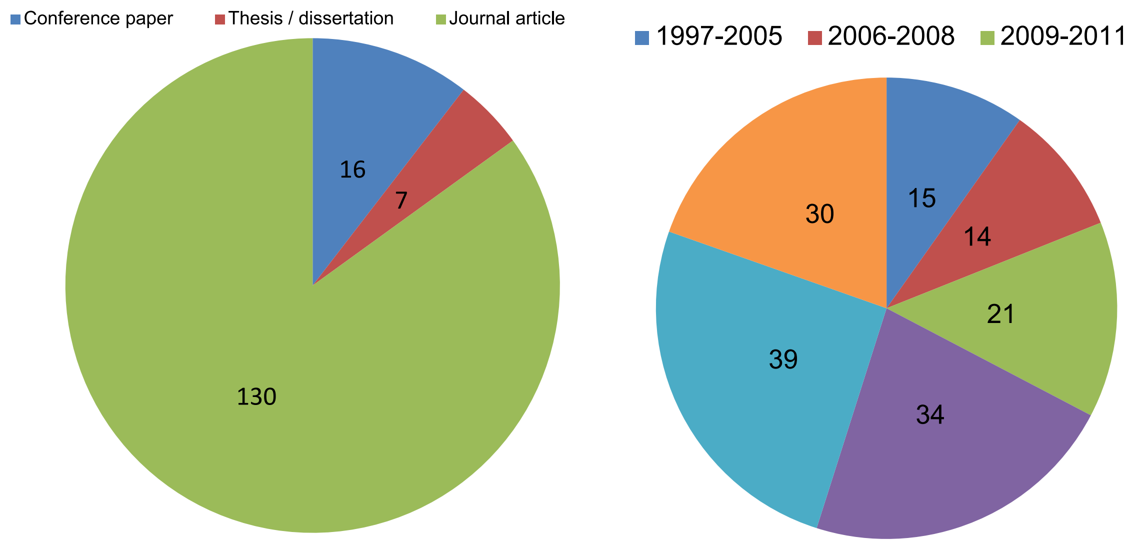

Fig. 4. The *meta*-analysis of the sources of the publications (left) and the year of publications in the database developed for the *Pre-bcc* regression model generation.

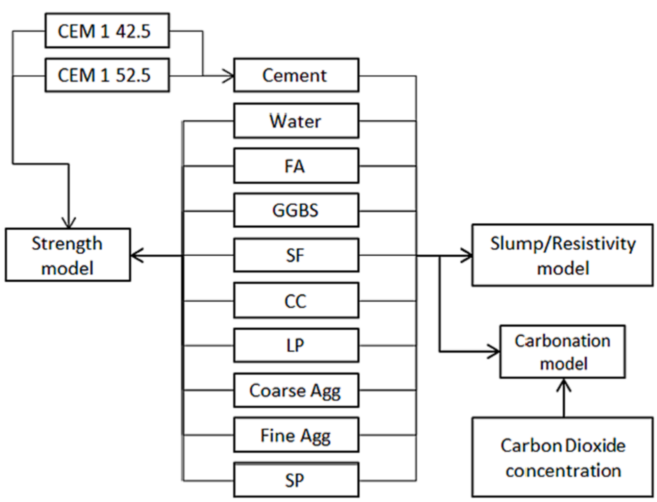

Fig. 5. A flow diagram of the number and name of the input variables for each of the models developed to predict each of the functional properties of BCC.

processing, the data associated with the candidate that has the lowest MSPE was then saved as the input data for the actual model generation ensuring that the output data was composed of disjoint subsets each of which can be adequately covered by a weak learner. This allowed using the same control flow for model generation and pre-processing (outlier detection), the difference being that model generation does not actually throw away any data.

3.2. Data collection

In order to build a statistically sound database for the four functional properties understudy, 1,683 data points were collected from published papers as shown in the supplementary materials I. The mixes were extracted from 153 journal articles published between 1997 and 2020 [4,8–13,16–18,21,26,29,36–39,53,58–59,67–197]. The composition and breakdown of the database is shown in Figs. 3 and 4. Note that the total number of the values represented in the pie charts differ from the total points surveyed since a SCM could have been tested against more than one property.

The online databases used were EThOS, Google scholar, SCOPUS, Science Direct and ResearchGate. The search words were different combinations of the names of the SCMs and the functional properties under investigation. The inclusion criteria were that: 1) the tests done on the concrete mixes were following the *ACI*, EN or RILEM standards, 2) the study is either a dissertation or a peer-reviewed article as a conference proceeding or a journal article and 3) the concrete mixes reported in the study include one or more of the SCMs and these were tested against one or more of the functional properties. In total, 12 input variables constitute the concrete mix. As shown in Fig. 5, for the strength model, as per the recommendations from the literature, the cement content was sub-divided into two sub-variables which indicate the cement strength (CEM I-42.5 and CEM I-52.5). In case the differentiation was not made in the original source, cement was assumed to be CEM I-42.5.

It is worth noting that an important feature in the *Pre-bcc* model is the ability to predict the carbonation rate of the BCC mix based on accelerated or natural carbonation experimental results. In order to convert the input data of the accelerated carbonation rate K_a to natural carbonation rate K_n, the Equation (2) is used, where CC_n is the natural carbon concentration, assumed to be 0.03 %, and CC_a is the carbon concentration inside the testing chamber (%) [64].

$$K_n = K_a\sqrt{\frac{CC_n}{CC_a}} \tag{2}$$

3.3. Model generation

The approach to the process of generating learners h_i at L1 as well as selecting the subset of samples S_i was not an off-the-self implementation. The intuition behind the approach is that the data used for *Pre-bcc* comes from different sources with potentially different conditions that may be difficult to fit together (especially in the presence of outliers when the model generation is used in pre-processing). Moreover, since multiple learners exist, each set of learners might be focusing on the data from a subset of sources $B_k \subset S$. However, if sources were randomly grouped, it is likely that some of the data subsets might be over or under fit. In line with the concept of boosting, where multiple weak learners are created in stages similar to the concept of gradient descent steps [198], a subroutine was implemented to develop subsequent learners by removing the sources that fit first so that when a learner h_i is found by using cross-validation grid search and fit on a subset S_i, only sources that have any elements above a certain error are used for the subsequent learner. If the coverage of the current h_i is below a certain amount, the model is rejected, and the algorithm terminates when the number of elements out of coverage is<10 % of the data. The algorithm terminates without

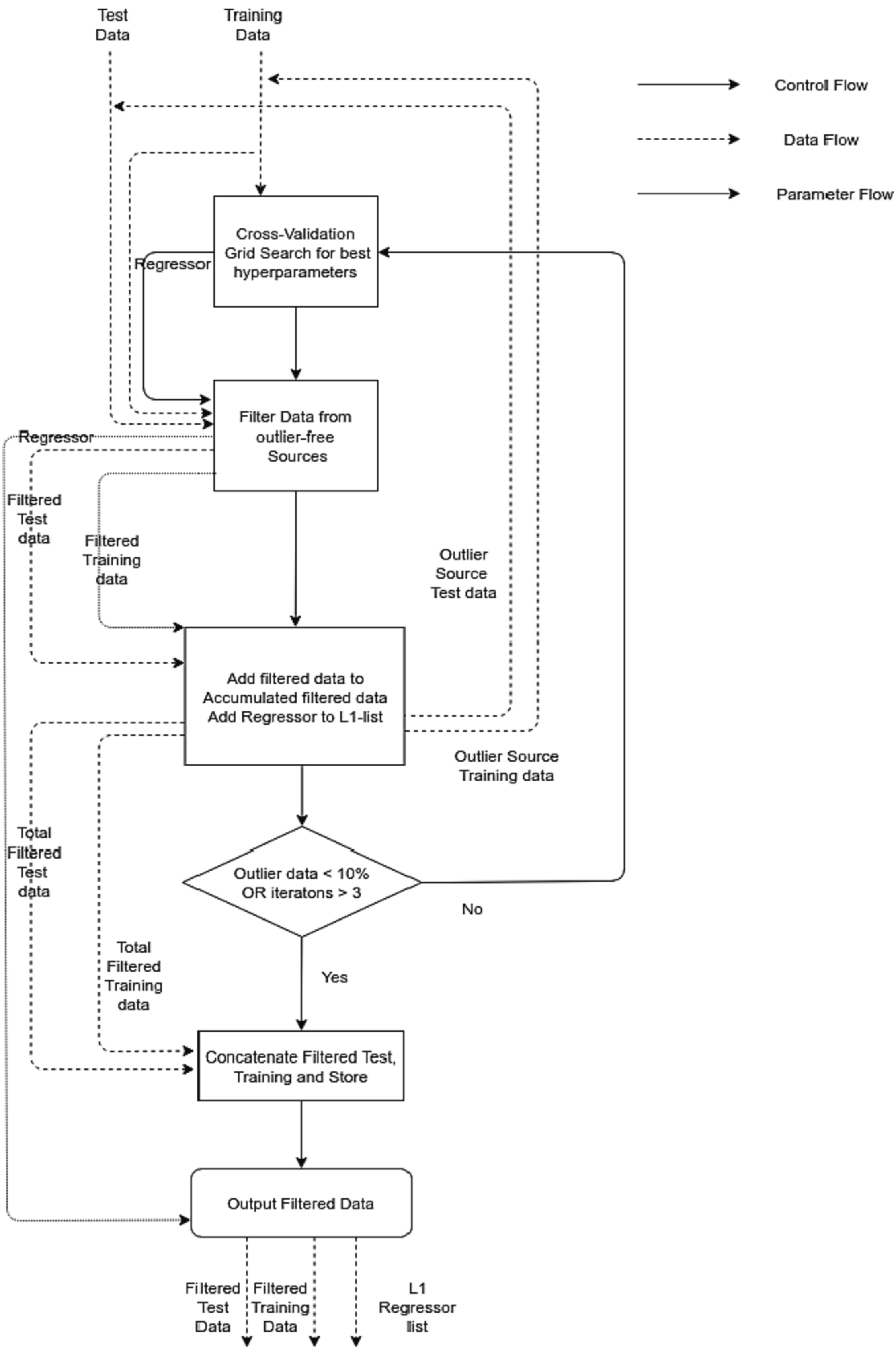

Fig. 6. A flow diagram showing the Pre-bcc regression model generation algorithm.

Table 6
The optimized learner type for level 2 of each regression model and its statistical performance.

Variable	L2 learner type	Training Size	Test Size	Statistical performance MSPE	MAPE	R
Slump	Random Forest	474	74	20.5 %	12.5 %	0.95
Strength	Bayesian Ridge	1090	212	12.0 %	9.0 %	0.96
Chloride	Random Forest	241	33	18.0 %	14.5 %	0.93
Carbonation	XGB	278	34	18.7 %	15.2 %	0.94

convergence if multiple iterations yield inadequate coverage, in which case the data is reshuffled, and the algorithm search for a new set of L1 models. The flow chart in Fig. 6 represents this process.

4. Results and discussions

The model selection process described above targets first the optimization of the learner type for the second level of the regression model. Table 6 shows the optimized learner type for level 2 of each model as well as the training/test data sizes and the statistical performance of the models. The prediction accuracy was measured using 3 different statistical metrics; MSPE as per equation (1), the mean absolute percentage error (MAPE) as in equation (3), and the correlation coefficient R which is the slope of the linear plot shown in Fig. 7 below. The plot compares the actual experimental values of the (testing data set) that was randomly separated at the data input stage (20 % of the database) against the predicted values using the regression models.

In Equation (3), n is the number of times the summation iteration happens, A_t is the true value and F_t is the predicted one:

$$MAPE = \frac{1}{n}\sum_{t=1}^{n}\left|\frac{A_t - F_t}{A_t}\right| \tag{3}$$

For each of the four target variables, the evaluation of the performance and behaviour of the regression models could be summarized as follows:

1. Fig. 7 shows the plot of the predictions vs actual values over the test dataset to visualize the goodness of the fits. As it can be seen, the models provide a suitable fit from the mix design point of view and the design governing variables. As it was expected, the parameters with more data present such as slump and strength, result in slightly better performing models in terms of accuracy of predictions ($R^2 = 0.9$) compared to chloride and carbonation ones ($R^2 = 0.88$).
2. In statistics and machine learning, the bias represents the ability of the learner to fit the given dataset. The higher the bias, the less reliable a prediction model is. An unbiased learner would converge to the mean of the dataset, so it would be expected that the residual error from the predictions are normally distributed with zero mean. Fig. 8 shows the plots of the residual error in each of the In the *Pre-bcc* models vs predictions over the entire set in order to provide a measure of bias. The models show unnoticeable bias since the residuals appear as a normal distribution with zero mean throughout the different regions of the data set. The slump variable does show bias since the residuals are mostly positive in the lower values of the prediction and mostly negative in the upper values. The bias is believed to be a result of a typical error in the nature of the sampling process for the slump data from the experimental database results. In a slump cone test, the researcher sometimes resort to the EN 206–01

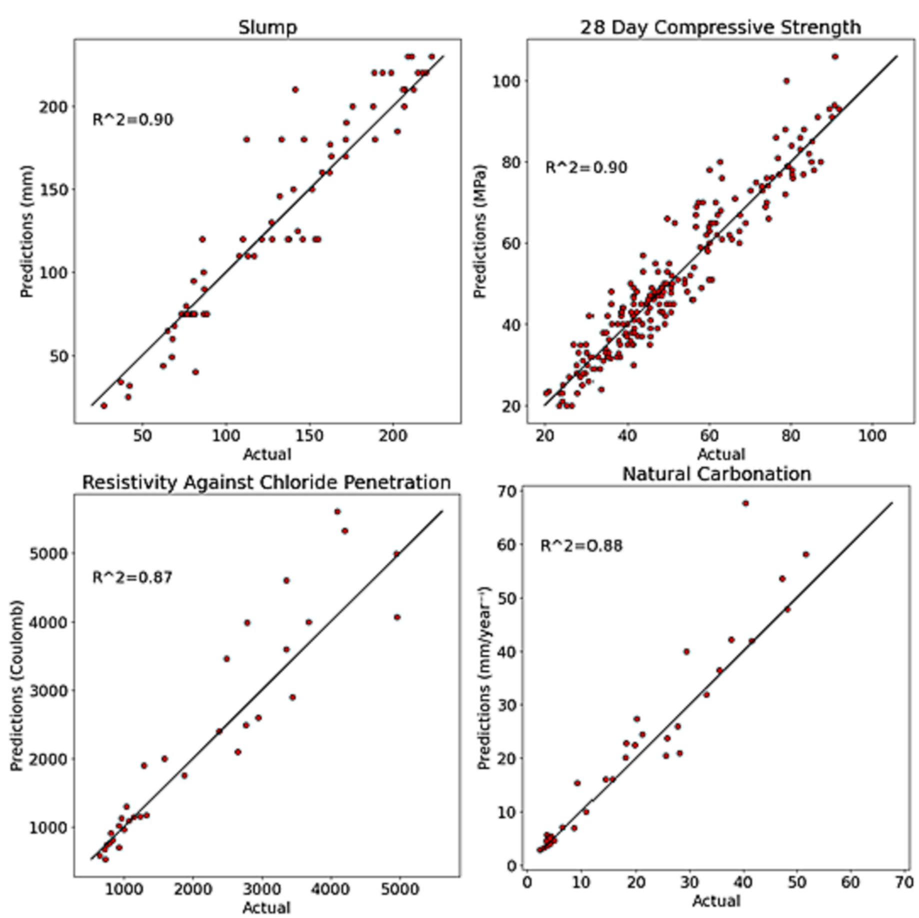

Fig. 7. Predicted vs actual values of the testing sample for the BCC functional parameters of the *Pre-bcc* prediction model.

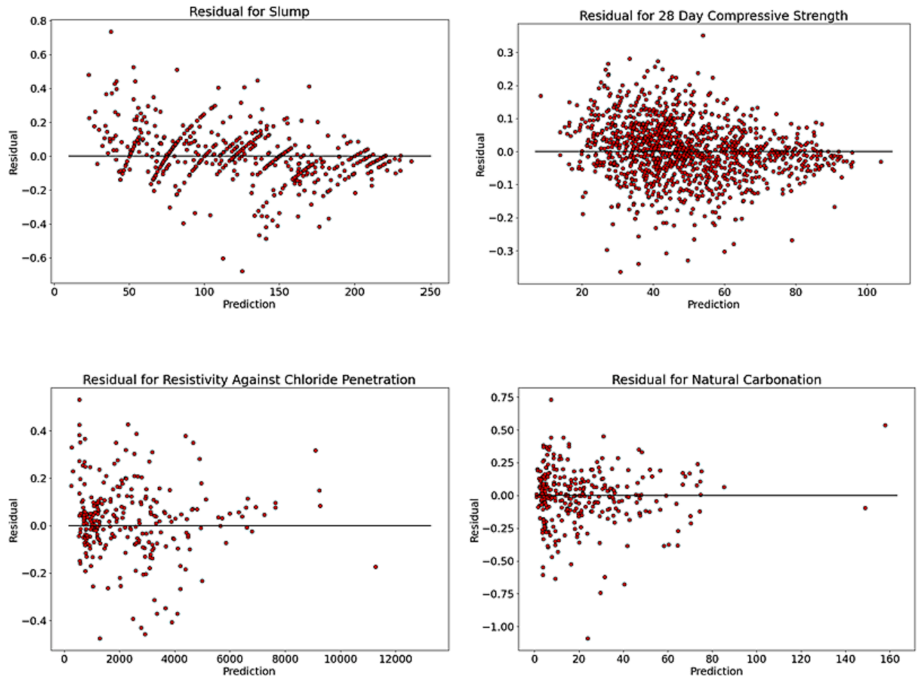

Fig. 8. The residual error across the four functional parameters of the *Pre-bcc* prediction models.

Table 7
The specific gravity of BCC mix constituents.

Water	Cement	FA	GGBS	SF	CC	LP	Coarse	Fine	SP
1	3.15	2.25	2.91	2.25	2.41	2.65	2.61	2.71	1.22

Table 8
Preferred range for each of the BCC mix constituents relative to the total binder content.

	Binder (kg/m^3)	Ratio of constituent to Binder Water	Cement	FA	GGBS	SF	LP	CC	Coarse	Fine	SP
Minimum	200	0.25	0.1	0	0	0	0	0	0.5	0.5	0
Maximum	600	1	1	0.5	0.9	0.15	0.2	0.5	5.5	5.5	0.02
Step	25	0.01	0.01	0.01	0.01	0.01	0.01	0.01	0.01	0.01	0.005

slump classes (S1, S2, S3, S4 and S5). While building the model, the average values were decided as representatives of these classes (20 mm, 75 mm, 120 mm, 180 mm and 250 mm) which could lead to the results being discrete rather than being a continuous range of values.

5. Model validation

5.1. Self –Validation

In order to validate the *Pre-bcc* model, a web-based tool was implemented at https://bcc-regression.online/login/?next=/predict/ [199]. This open-accessed platform hence allows users to test the claimed capabilities and accuracy of the model. After registering, using a valid email address, a user is allowed to enter, any BCC mix that follows the logical constraint that the summation of the volume of all mix constituents in a unit volume of concrete equals to 1.0, can be analysed. The volume unity constraint is calculated by the tool through assuming the specific gravity values reported in Table 7 for each concrete constituent.

The user is allowed to enter the mixing proportions either by weight, or through choosing the ratios tab, the total value for the binder and the ratio of each of the remaining constituents to the binder by weight as well. BCC mixes entered by the user should also fulfil the range shown in Table 8 for each constituent to remain within the data range found in the databases -through which the model was developed.

A check of the mix can be performed to ensure that the values entered, whether by mass or by ratios, are compliant with both constraints: the unity volume in Table 7 and the preferred range of values for each constituent in Table 8. Upon initiating the check of the mix, the tool would inform the user whether the mix passes requirements and recommendations or an error message would be displayed and the user asked to re-enter a compliant mix.

The user is expected, after checking the mix, to click “initiate the calculation” in order to produce the values for the slump (in mm), 28-day compressive strength (in MPa), the resistivity against chloride ingress (in Coulombs) and natural carbonation rate (in $mm/year^{-1}$). The values are presented to the user numerically. The tool can also extract the closest mix from the database in terms of mixing proportions and the values that were recorded for each of the functional performances to allow the user to compare those with the obtained values from *Pre-bcc*.

5.2. Comparison against previous models

Comparing *Pre-bcc* regression model developed in this paper against the average values of the statistical accuracy of the regression models reviewed from the literature in Table 4 and 5 shows that although the *Pre-bcc* model was developed using more data points compared to the

Table 9
A comparison between the statistical performance *Pre-bcc* and the average of the literature models.

Author	Property	Statistical accuracy	
		R	MAPE (%)
Literature average	Slump	0.98	2.53
Pre-bcc		0.95	12.5
Literature average	Strength	0.98	7.77
Pre-bcc		0.96	9.01
Literature average	Chloride Resistivity	0.96	7.89
Pre-bcc		0.93	14.5
Literature average	Carbonation	0.96	5.04
Pre-bcc		0.94	15.2

others, the statistical accuracy is slightly lower as shown in Table 9. However, the comparison would be unrepresentative because the average from the literature is insufficient for indicating the superior performance of a certain model compared to *Pre-bcc*. More importantly, the advantage of the newly developed model is that it combines, for the first time, with solid statistical accuracy the four functional properties most significant in concrete research for varying percentages of replacement of OPC with all five prominent SCMs.

5.3. Further development of the model

Similar to any data-sensitive model such as *Pre-bcc*, it is always recommended to increase the input database in order to enhance the reliability and statistical accuracy of the predictions. Hence, it is a work in progress to create an open-access database to which researchers could contribute their empirical experimental findings on any of the BCC mixes under study for any of the four properties. Nevertheless, the model has, up to date, dealt with SCMs as materials with homogenous chemical and physical characterization and accordingly reactivity while in reality they could vary widely depending on the source. Accordingly, the next stage of the model would be predict the concrete properties based on pozzolanic reactivity parameters such as R^3 test reactivity or Frattini result.

6. Conclusions

The extensive literature review carried out highlights the urgent need for approaches enabling the prediction the functional performance of BCC mixes. The conclusions drawn from the study are as follows:

1. The newly developed *Pre-bcc* regression model is the first, to the best of the authors' knowledge, to predict the slump, strength and resistance to chloride ingress and carbonation for BCC mixes based on all five considered SCMs.
2. The model includes filters to avoid the biases in selecting data from the same source as well as optimizing the selection of the type of learner which guarantees a reliable prediction result.
3. As it stands, the model achieves, for the wide range explained, an average statistical accuracy of 0.96 for R value and 5 % for MAPE.
4. The model guarantees a reliable, highly accurate prediction of the mechanical and durability performance of blended cement concrete mixes.
5. The *Pre-bcc* regression model is the first, to the best of the authors' knowledge to provide the users with an open-access tool to validate the model and implement it in their own studies via this link: https://bcc-regression.online/login/?next=/predict/

Finally, the biggest contribution of the model is its ability to act as a screening tool for researchers and concrete producers to optimize the size of their experimental campaigns through accurately and reliably predicting the performance of BCC mixes in an attempt to reach a sustainable concrete alternative.

Declaration of Competing Interest

The authors declare that they have no known competing financial interests or personal relationships that could have appeared to influence the work reported in this paper.

Data availability

The data was shared as Data in Brief

Acknowledgments

The authors acknowledge no conflict of interest.

Appendix A. Supplementary data

Supplementary data to this article can be found online at https://doi.org/10.1016/j.conbuildmat.2022.129019.

References

[1] M.K. Mohan, A.V. Rahul, B. van Dam, T. Zeidan, G. De Schutter, K. Van Tittelboom, Performance criteria, environmental impact and cost assessment for 3D printable concrete mixtures, Resources, Conservation and Recycling 181 (2022), 106255.
[2] H. Hafez, R. Kurda, N. Al-Ayish, T. Garcia-Segura, W.M. Cheung, B. Nagaratnam, A whole life cycle performance-based ECOnomic and ECOlogical assessment framework (ECO2) for concrete sustainability, Journal of Cleaner Production 292 (2021), 126060.
[3] S.A. Miller, Supplementary cementitious materials to mitigate greenhouse gas emissions from.concrete: can there be too much of a good thing? Journal of Cleaner Production 178 (2018) 587–598.
[4] H. Fitriani, A. Ahmed, O. Kolawole, F. Hyndman, Y. Idris, R. Rosidawani, Optimizing Compressive Strength Properties of Binary Blended Cement Rice Husk Concrete for Road Pavement, Trends in Sciences 19 (9) (2022).
[5] T. Hanein, K.C. Thienel, F. Zunino, A. Marsh, M. Maier, B. Wang, M. Canut, M. C. Juenger, M. Ben Haha, F. Avet, A. Parashar, Clay calcination technology: state-of-the-art review by the RILEM TC 282-CCL, Materials and Structures 55 (1) (2022) 1–29.
[6] Al-Jamimi, H.A., Al-Kutti, W.A., Alwahaishi, S. and Alotaibi, K.S., 2022. Prediction of Compressive Strength in Plain and Blended Cement Concretes Using a Hybrid Artificial Intelligence Model. *Case Studies in Construction Materials*, p. e01238.
[7] M.C. Juenger, R. Snellings, S.A. Bernal, Supplementary cementitious materials: New sources, characterization, and performance insights, Cement and Concrete Research 122 (2019) 257–273.
[8] M.M. Johari, J.J. Brooks, S. Kabir, P. Rivard, Influence of supplementary cementitious materials on engineering properties of high strength concrete, Construction and Building Materials 25 (5) (2011) 2639–2648.
[9] C.S. Poon, S.C. Kou, L. Lam, Compressive strength, chloride diffusivity and pore structure of high performance metakaolin and silica fume concrete, Construction and building materials 20 (10) (2006) 858–865.
[10] K.-R. Wu, B. Chen, W. Yao, D. Zhang, Effect of coarse aggregate type on mechanical properties of high-performance concrete, Cement and Concrete Research 31 (2001) 1421–1425.
[11] B.S. Divsholi, T.Y.D. Lim, S. Teng, Durability properties and microstructure of ground granulated blast furnace slag cement concrete, International Journal of Concrete Structures and Materials 8 (2) (2014) 157–164.
[12] W. Wongkeo, P. Thongsanitgarn, A. Ngamjarurojana, A. Chaipanich, Compressive strength and chloride resistance of self-compacting concrete containing high level fly ash and silica fume, Materials & Design 64 (2014) 261–269.
[13] X.Y. Wang, Simulation for optimal mixture design of low-CO_2 high-volume fly ash concrete considering climate change and CO_2 uptake, Cement and Concrete Composites 104 (2019), 103408.
[14] A.A. Ramezanianpour, H.B. Jovein, Influence of metakaolin as supplementary cementing material on strength and durability of concretes, Construction and Building materials 30 (2012) 470–479.
[15] C.F. Lu, W. Wang, Q.T. Li, M. Hao, Y. Xu, Effects of micro-environmental climate on the carbonation depth and the pH value in fly ash concrete, Journal of Cleaner Production 181 (2018) 309–317.
[16] Y. Zhang, J. Zhang, M. Lü, J. Wang, Y. Gao, April. Considering uncertainty in life-cycle carbon dioxide emissions of fly ash concrete Vol. 172(4 (2018) 198–206.
[17] M.S. Meddah, M.C. Lmbachiya, R.K. Dhir, Potential use of binary and composite limestone cements in concrete production, Construction and Building Materials 58 (2014) 193–205.
[18] B. Felekoğlu, S. Türkel, B. Baradan, Effect of water/cement ratio on the fresh and hardened properties of self-compacting concrete, Building and Environment 42 (2007) 1795–1802.

[19] V. Chandwani, V. Agrawal, R. Nagar, Modeling slump of ready mix concrete using genetic algorithms assisted training of Artificial Neural Networks, Expert Systems With Applications 42 (2015) 885–893.
[20] H. Moayedi, B. Kalantar, L.K. Foong, D. Tien Bui, A. Motevalli, Application of three metaheuristic techniques in simulation of concrete slump, Applied Sciences 9 (20) (2019) 4340.
[21] S. Teng, T.Y.D. Lim, B.S. Divsholi, Durability and mechanical properties of high strength concrete incorporating ultra fine ground granulated blast-furnace slag, Construction and Building Materials 40 (2013) 875–881.
[22] Z. Giergiczny, Fly ash and slag, Cement and Concrete Research 124 (2019), 105826.
[23] R. Kurda, J. De Brito, J. Silvestre, CONCRETop - A multi-criteria decision method for concrete optimization, Environmental Impact Assessment Review 74 (2019) 73.
[24] A.K. Al-Shamiri, J.H. Kim, T.F. Yuan, Y.S. Yoon, Modeling the compressive strength of high-strength concrete: An extreme learning approach, Construction and Building Materials 208 (2019) 204–219.
[25] D. Sathyan, K.B. Anand, Influence of superplasticizer family on the durability characteristics of fly ash incorporated cement concrete, Construction and Building Materials 204 (2019) 864–874.
[26] R.A. Einsfeld, M.S.L. Velasco, Fracture parameters for high-performance concrete, Cement and Concrete Research 36 (2006) 576–583.
[27] F. Hedayatinia, M. Delnavaz, S.S. Emamzadeh, Rheological properties, compressive strength and life cycle assessment of self-compacting concrete containing natural pumice pozzolan, Construction and Building Materials 206 (2019) 122–129.
[28] B. Lothenbach, K. Scrivener, R.D. Hooton, Supplementary cementitious materials, Cement and concrete research 41 (12) (2011) 1244–1256.
[29] D.K. Panesar, R. Zhang, Performance comparison of cement replacing materials in concrete: Limestone fillers and supplementary cementing materials–A review, Construction and Building Materials 251 (2020), 118866.
[30] K.L. Scrivener, V.M. John, E.M. Gartner, Eco-efficient cements: Potential economically viable solutions for a low-CO_2 cement-based materials industry, Cement and Concrete Research 114 (2018) 2–26.
[31] S. Sui, F. Georget, H. Maraghechi, W. Sun, K. Scrivener, Towards a generic approach to durability: Factors affecting chloride transport in binary and ternary cementitious materials, Cement and Concrete Research 124 (2019), 105783.
[32] V. Garcia, R. François, M. Carcasses, P. Gegout, Potential measurement to determine the chloride threshold concentration that initiates corrosion of reinforcing steel bar in slag concretes, Materials and structures 47 (9) (2014) 1483–1499.
[33] W.V. Srubar III, Stochastic service-life modeling of chloride-induced corrosion in recycled-aggregate concrete, Cement and Concrete Composites 55 (2015) 103–111.
[34] S. Mahima, P. Moorthi, A. Bahurudeen, A. Gopinath, Influence of chloride threshold value in service life prediction of reinforced concrete structures, Sādhanā 43 (2018) 1–19.
[35] J. Sun, Z. Chen, Influences of limestone powder on the resistance of concretes to the chloride ion penetration and sulfate attack, Powder Technology 338 (2018) 725–733.
[36] S. Kumar, B. Rai, R. Biswas, P. Samui, D. Kim, Prediction of rapid chloride permeability of self-compacting concrete using Multivariate Adaptive Regression Spline and Minimax Probability Machine Regression, Journal of Building Engineering 32 (2020), 101490.
[37] R.G. Pillai, R. Gettu, M. Santhanam, S. Rengaraju, Y. Dhandapani, S. Rathnarajan, A.S. Basavaraj, Service life and life cycle assessment of reinforced concrete systems with limestone calcined clay cement (LC3), Cement and Concrete Research 118 (2019) 111–119.
[38] P. Van den Heede, M. De Schepper, N. De Belie, Accelerated and natural carbonation of concrete with high volumes of fly ash: chemical, mineralogical and microstructural effects, Royal Society open science 6 (1) (2019), 181665.
[39] D. Panesar, K. Seto, C. Churchill, Impact of the selection of functional unit on the life cycle assessment of green concrete, The International Journal of Life Cycle Assessment 22 (2017) 1969–1986.
[40] S. Bernal, R. San Nicolas, J. Provis, R. Mejía De Gutiérrez, J. Van Deventer, Natural carbonation of aged alkali-activated slag concretes, Materials and Structures 47 (2014) 693–707.
[41] C.Q. Lye, R.K. Dhir, G.S. Ghataora, Carbonation resistance of GGBS concrete, Magazine of Concrete Research 68 (18) (2016) 936–969.
[42] S. Kandasami, T.A. Harrison, M.R. Jones, G. Khanna, Benchmarking UK concretes using an accelerated carbonation test, Magazine of concrete research 64 (8) (2012) 697–706.
[43] M.S. Meddah, M.A. Ismail, S. El-Gamal, H. Fitriani, Performances evaluation of binary concrete designed with silica fume and metakaolin, Construction and Building Materials 166 (2018) 400–412.
[44] B. Ali, H. Ahmed, L. Ali Qureshi, R. Kurda, H. Hafez, H. Mohammed, A. Raza, Enhancing the hardened properties of recycled concrete (RC) through synergistic incorporation of fiber reinforcement and silica fume, Materials 13 (18) (2020) 4112.
[45] J. de la Cruz, I. Segura, P. Pujadas, J.M. Torrents, A. de la Fuente, Non-destructive test approach for assessing the amount of fibre in polymeric fibre reinforced concrete, Construction and Building Materials 317 (2022), 125964.
[46] N. Tošić, S. Aidarov, A. de la Fuente, Systematic review on the creep of fiber-reinforced concrete, Materials 13 (22) (2020) 5098.
[47] Q.F. Liu, M.F. Iqbal, J. Yang, X.Y. Lu, P. Zhang, M. Rauf, Prediction of chloride diffusivity in concrete using artificial neural network: Modelling and performance evaluation, Construction and Building Materials 268 (2021), 121082.
[48] J. Pinkse, M. Dommisse, Overcoming barriers to sustainability: an explanation of residential builders' reluctance to adopt clean technologies, Business Strategy and the Environment 18 (8) (2009) 515–527.
[49] M. Ozturan, B.I.R.G.Ü.L. Kutlu, T. Ozturan, Comparison of concrete strength prediction techniques with artificial neural network approach, Building research journal 56 (1) (2008) 23–36.
[50] E.M. Golafshani, A. Behnood, M. Arashpour, Predicting the compressive strength of normal and High-Performance Concretes using ANN and ANFIS hybridized with Grey Wolf Optimizer, Construction and Building Materials 232 (2020), 117266.
[51] Hoang, N.D. and Pham, A.D., 2016. Estimating Concrete Workability Based on Slump Test with Least Squares Support Vector Regression. *Journal of Construction Engineering*, *2016*.
[52] Cihan, M.T., 2019. Prediction of Concrete Compressive Strength and Slump by Machine Learning Methods. *Advances in Civil Engineering*, *2019*.
[53] L. Chen, C.H. Kou, S.W. Ma, Prediction of slump flow of high-performance concrete via parallel hyper-cubic gene-expression programming, Engineering Applications of Artificial Intelligence 34 (2014) 66–74.
[54] https://scikit-learn.org/stable/index.html.
[55] H. Naseri, H. Jahanbakhsh, P. Hosseini, F.M. Nejad, Designing sustainable concrete mixture by developing a new machine learning technique, Journal of Cleaner Production 258 (2020), 120578.
[56] Y. Yu, W. Li, J. Li, T.N. Nguyen, A novel optimised self-learning method for compressive strength prediction of high performance concrete, Construction and Building Materials 184 (2018) 229–247.
[57] N. Ghafoori, M. Najimi, J. Sobhani, M.A. Aqel, Predicting rapid chloride permeability of self-consolidating concrete: a comparative study on statistical and neural network models, Construction and Building Materials 44 (2013) 381–390.
[58] S. Inthata, W. Kowtanapanich, R. Cheerarot, Prediction of chloride permeability of concretes containing ground pozzolans by artificial neural networks, Materials and structures 46 (10) (2013) 1707–1721.
[59] O.A. Mohamed, M. Ati, W. Al Hawat, Implementation of Artificial Neural Networks for Prediction of Chloride Penetration in Concrete. *International Journal of*, Engineering & Technology 7 (2.28) (2018) 47–52.
[60] M. Najimi, N. Ghafoori, M. Nikoo, Modeling chloride penetration in self-consolidating concrete using artificial neural network combined with artificial bee colony algorithm, Journal of Building Engineering 22 (2019) 216–226.
[61] E.F. Felix, E. Possan, R. Carrazedo, Analysis of training parameters in the ANN learning process to mapping the concrete carbonation depth, Journal of Building Pathology and Rehabilitation 4 (1) (2019) 1–13.
[62] Y. Kellouche, B. Boukhatem, M. Ghrici, A. Tagnit-Hamou, Exploring the major factors affecting fly-ash concrete carbonation using artificial neural network, Neural Computing and Applications 31 (2) (2019) 969–988.
[63] D. Luo, D. Niu, Z. Dong, Application of neural network for concrete carbonation depth prediction, Purdue University, International conference on durability of concrete, 2014.
[64] W.Z. Taffese, E. Sistonen, J. Puttonen, CaPrM: Carbonation prediction model for reinforced concrete using machine learning methods, Construction and Building Materials 100 (2015) 70–82.
[65] J. Mendes-Moreira, C. Soares, A.M. Jorge, J.F.D. Sousa, Ensemble approaches for regression: A survey, Acm computing surveys (csur) 45 (1) (2012) 1–40.
[67] P. Van den Heede, M. De Keersmaecker, A. Elia, A. Adriaens, N. De Belie, Service life and global warming potential of chloride exposed concrete with high volumes of fly ash, Cement and Concrete Composites 80 (2017) 210–223.
[68] Adam, A.A., Molyneaux, T.C.K., Patnaikuni, I. and Law, D.W., 2009. Strength, sorptivity and carbonation in blended OPC-GGBS, alkali activated slag, and fly ash based geopolymer concrete.
[69] U.z. Zaman, Development of Sustainable and Low Carbon Concretes for the Gulf Environment.PhD dissertation, University of Bath, 2014.
[70] O.S.B. Al-Amoudi, W.A. Al-Kutti, S. Ahmad, M. Maslehuddin, Correlation between compressive strength and certain durability indices of plain and blended cement concretes, Cement and Concrete Composites 31 (9) (2009) 672–676.
[71] Y. Alhassan, Y. Ballim, An Experimental Study On Carbonation Of Plain And Blended Cement Concrete, International Journal of Scientific & Technology Research 6 (2017) 436–443.
[72] E.O. Amankwah, M. Bediako, C.K. Kankam, Influence of calcined clay pozzolana on strength characteristics of Portland cement concrete, International Journal of Material Science Applications 3 (2014) 410.
[73] D.E. Angulo-Ramirez, R.M. de Gutiérrez, W.G. Valencia-Saavedra, M.H.F. De Medeiros, J. Hoppe-Filho, Carbonation of hybrid concrete with high blast furnace slag content and its impact on structural steel corrosion, Materiales de Construcción 69 (333) (2019) 182.
[74] V.V. Arora, B. Singh, V. Patel, Durability and corrosion studies in prestressed concrete made with blended cement, Journal of Asian Concrete Federation 5 (1) (2019) 15–24.
[75] C.D. Atiş, Accelerated carbonation and testing of concrete made with fly ash, Construction and Building Materials 17 (3) (2003) 147–152.
[76] B. Balakrishnan, A.A. Awal, Durability properties of concrete containing high volume Malaysian fly ash, Measurement 2 (2.94) (2014) 2–94.
[77] B. Baten, Effect of blended cement on service life enhancement of concrete structures in marine environment, Bangladesh University of Engineering and Technology, 2019. Masters dissertation.

[78] M.L. Berndt, Properties of sustainable concrete containing fly ash, slag and recycled concrete aggregate, Construction and building materials 23 (7) (2009) 2606–2613.
[79] C. Bilim, C.D. Atiş, H. Tanyildizi, O. Karahan, Predicting the compressive strength of ground granulated blast furnace slag concrete using artificial neural network, Advances in Engineering Software 40 (5) (2009) 334–340.
[80] W.K. Biswas, Y. Alhorr, K.K. Lawania, P.K. Sarker, E. Elsarrag, Life cycle assessment for environmental product declaration of concrete in the Gulf States, Sustainable Cities and Society 35 (2017) 36–46.
[81] R. Bucher, P. Diederich, G. Escadeillas, M. Cyr, Service life of metakaolin-based concrete exposed to carbonation: Comparison with blended cement containing fly ash, blast furnace slag and limestone filler, Cement and Concrete Research 99 (2017) 18–29.
[82] D. Burden, The durability of concrete containing high levels of fly ash (No. PCA R&D Serial, No. 2989), University of New Brunswick, Department of Civil Engineering, 2006.
[83] K. Buss, Ternary combination concretes using GGBS, fly ash & limestone, University of Dundee, Dundee, UK, 2013. Doctoral dissertation, PhD Thesis.
[84] K. Celik, C. Meral, A.P. Gursel, P.K. Mehta, A. Horvath, P.J. Monteiro, Mechanical properties, durability, and life-cycle assessment of self-consolidating concrete mixtures made with blended portland cements containing fly ash and limestone powder, Cement and Concrete Composites 56 (2015) 59–72.
[85] A. Gholampour, T. Ozbakkaloglu, Performance of sustainable concretes containing very high volume Class-F fly ash and ground granulated blast furnace slag, Journal of Cleaner Production 162 (2017) 1407–1417.
[86] Collepardi, M., Collepardi, S., Olagot, J.O. and Simonelli, F., 2004, May. The influence of slag and fly ash on the carbonation of concrete. In *Proc. of 8th CANMET/ACI Int. Conf. on Fly Ash, Silica Fume, Slag, and Natural Pozzolans in Concrete, held May* (pp. 23-29).
[87] L.K. Crouch, R. Hewitt, B. Byard, High volume fly ash concrete, World of Coal Ash (WOCA) (2007) 1–14.
[88] L. Czarnecki, P. Woyciechowski, G. Adamczewski, Risk of concrete carbonation with mineral industrial by-products, KSCE Journal of Civil Engineering 22 (2) (2018) 755–764.
[89] Y. Dhandapani, T. Sakthivel, M. Santhanam, R. Gettu, R.G. Pillai, Mechanical properties and durability performance of concretes with Limestone Calcined Clay Cement (LC3), Cement and Concrete Research 107 (2018) 136–151.
[90] B.S. Dhanya, M. Santhanam, R. Gettu, R.G. Pillai, Performance evaluation of concretes having different supplementary cementitious material dosages belonging to different strength ranges, Construction and Building Materials 187 (2018) 984–995.
[91] A.M. Diab, M. Abd Elmoaty, A.A. Aly, Long term study of mechanical properties, durability and environmental impact of limestone cement concrete, Alexandria Engineering Journal 55 (2) (2016) 1465–1482.
[92] P. Dinakar, K.G. Babu, M. Santhanam, Corrosion behaviour of blended cements in low and medium strength concretes, Cement and Concrete Composites 29 (2) (2007) 136–145.
[93] P. Dinakar, K.P. Sethy, U.C. Sahoo, Design of self-compacting concrete with ground granulated blast furnace slag, Materials & Design 43 (2013) 161–169.
[94] P. Duan, Z. Shui, W. Chen, C. Shen, Enhancing microstructure and durability of concrete from ground granulated blast furnace slag and metakaolin as cement replacement materials, Journal of Materials Research and Technology 2 (1) (2013) 52–59.
[95] A. Duran-Herrera, J.M. Mendoza-Rangel, E.U. De-Los-Santos, F. Vazquez, P. Valdez, D.P. Bentz, Accelerated and natural carbonation of concretes with internal curing and shrinkage/viscosity modifiers, Materials and Structures 48 (4) (2015) 1207–1214.
[96] K. Eguchi, K. Takewaka, T. Yamaguchi, N. Ueda, A study on durability of blast furnace slag cement concrete mixed with metakaolin-based artificial pozzolan in actual marine environment, In *Third International Conference on Sustainable Construction Materials and* (2013). Technologies.
[97] F. Faleschini, M.A. Zanini, K. Brunelli, C. Pellegrino, Valorization of co-combustion fly ash in concrete production, Materials & Design 85 (2015) 687–694.
[98] H. Fanghui, W. Qiang, F. Jingjing, The differences among the roles of ground fly ash in the paste, mortar and concrete, Construction and Building Materials 93 (2015) 172–179.
[99] B. Felekoğlu, S. Türkel, B. Baradan, Effect of water/cement ratio on the fresh and hardened properties of self-compacting concrete, Building and Environment 42 (4) (2007) 1795–1802.
[100] M.R. Garcez, A.B. Rohden, L.G.G. de Godoy, The role of concrete compressive strength on the service life and life cycle of a RC structure: Case study, Journal of Cleaner Production 172 (2018) 27–38.
[101] T. García-Segura, V. Yepes, J. Alcalá, Life cycle greenhouse gas emissions of blended cement concrete including carbonation and durability, The International Journal of Life Cycle Assessment 19 (1) (2014) 3–12.
[102] M. Gesoğlu, E. Güneyisi, E. Özbay, Properties of self-compacting concretes made with binary, ternary, and quaternary cementitious blends of fly ash, blast furnace slag, and silica fume, Construction and Building Materials 23 (5) (2009) 1847–1854.
[103] R. Gettu, R.G. Pillai, M. Santhanam, A.S. Basavaraj, S. Rathnarajan, B.S. Dhanya, Sustainability-based decision support framework for choosing concrete mixture proportions, Materials and structures 51 (6) (2018) 1–16.
[104] G.L. Golewski, Green concrete composite incorporating fly ash with high strength and fracture toughness, Journal of cleaner production 172 (2018) 218–226.
[105] E. Güneyisi, M. Gesoğlu, E. Özbay, Strength and drying shrinkage properties of self-compacting concretes incorporating multi-system blended mineral admixtures, Construction and Building Materials 24 (10) (2010) 1878–1887.
[106] T.A. Harrison, M.R. Jones, M.D. Newlands, S. Kandasami, G. Khanna, Experience of using the prTS 12390–12 accelerated carbonation test to assess the relative performance of concrete, Magazine of Concrete Research 64 (8) (2012) 737–747.
[107] R.A. Hawileh, J.A. Abdalla, F. Fardmanesh, P. Shahsana, A. Khalili, Performance of reinforced concrete beams cast with different percentages of GGBS replacement to cement, Archives of Civil and Mechanical Engineering 17 (2017) 511–519.
[108] Holt, E., Kuosa, H., Leivo, M., Al-Neshawy, F., Piironen, J. and Sistonen, E., 2010. Accounting for coupled deterioration mechanisms for durable concrete containing mineral by-products. In *Proceedings of the 2nd International Conference on Sustainable Construction Materials and Technologies, Ancona, Italy* (Vol. 3, pp. 1631-1643).
[109] H.S. Shi, B.W. Xu, X.C. Zhou, Influence of mineral admixtures on compressive strength, gas permeability and carbonation of high performance concrete, Construction and Building Materials 23 (5) (2009) 1980–1985.
[110] K. Hussain, P. Choktaweekarn, S. Tangtermsirikul, Effect of mineral admixtures on curing sensitivity of concrete, Science & Technology Asia (2011) 1–8.
[111] M. Jalal, A. Pouladkhan, O.F. Harandi, D. Jafari, Comparative study on effects of Class F fly ash, nano silica and silica fume on properties of high performance self compacting concrete, Construction and Building Materials 94 (2015) 90–104.
[112] W.C. Jau, C.W. Fu, C.T. Yang, May. Study of feasibility and mechanical properties for producing high-flowing concrete with recycled coarse aggregates, in: In *International workshop on sustaInable development and concrete technology. BeijIng*, 2004, pp. 89–102.
[113] L. Jiang, Z. Liu, Y. Ye, Durability of concrete incorporating large volumes of low-quality fly ash, Cement and Concrete Research 34 (8) (2004) 1467–1469.
[114] M.R. Jones, R.K. Dhir, B.J. Magee, Concrete containing ternary blended binders: resistance to chloride ingress and carbonation, Cement and Concrete Research 27 (6) (1997) 825–831.
[115] K. Kaewmanee, S. Tangtermsirikul, Properties of binder systems containing cement, fly ash and limestone powder, Songklanakarin Journal of Science and Technology 36 (5) (2014) 569–576.
[116] O. Karahan, Transport properties of high volume fly ash or slag concrete exposed to high temperature, Construction and Building Materials 152 (2017) 898–906.
[117] S.K. Karri, G.R. Rao, P.M. Raju, Strength and durability studies on GGBS concrete, SSRG *International Journal of Civil Engineering* 2 (10) (2015) 34–41.
[118] O.R. Kavitha, V.M. Shanthi, G.P. Arulraj, V.R. Sivakumar, Microstructural studies on eco-friendly and durable Self-compacting concrete blended with metakaolin, Applied Clay Science 124 (2016) 143–149.
[119] Y. Khodair, B. Bommareddy, Self-consolidating concrete using recycled concrete aggregate and high volume of fly ash, and slag, Construction and Building Materials 153 (2017) 307–316.
[120] A. Khodabakhshian, J. De Brito, M. Ghalehnovi, E.A. Shamsabadi, Mechanical, environmental and economic performance of structural concrete containing silica fume and marble industry waste powder, Construction and Building Materials 169 (2018) 237–251.
[121] J. Khunthongkeaw, S. Tangtermsirikul, T. Leelawat, A study on carbonation depth prediction for fly ash concrete, Construction and building materials 20 (9) (2006) 744–753.
[122] S.C. Kou, C.S. Poon, D. Chan, Influence of fly ash as cement replacement on the properties of recycled aggregate concrete, Journal of materials in civil engineering 19 (9) (2007) 709–717.
[123] S.C. Kou, C.S. Poon, F. Agrela, Comparisons of natural and recycled aggregate concretes prepared with the addition of different mineral admixtures, Cement and Concrete Composites 33 (8) (2011) 788–795.
[124] R. Kurda, J.D. Silvestre, J. de Brito, Life cycle assessment of concrete made with high volume of recycled concrete aggregates and fly ash, Resources, Conservation and Recycling 139 (2018) 407–417.
[125] S. Lee, W. Park, H. Lee, Life cycle CO2 assessment method for concrete using CO2 balance and suggestion to decrease LCCO2 of concrete in South-Korean apartment, Energy and Buildings 58 (2013) 93–102.
[126] A. Leemann, P. Nygaard, J. Kaufmann, R. Loser, Relation between carbonation resistance, mix design and exposure of mortar and concrete, Cement and Concrete Composites 62 (2015) 33–43.
[127] H.Y. Leung, J. Kim, A. Nadeem, J. Jaganathan, M.P. Anwar, Sorptivity of self-compacting concrete containing fly ash and silica fume, Construction and Building Materials 113 (2016) 369–375.
[128] C. Lima, A. Caggiano, C. Faella, E. Martinelli, M. Pepe, R. Realfonzo, Physical properties and mechanical behaviour of concrete made with recycled aggregates and fly ash, Construction and Building Materials 47 (2013) 547–559.
[129] M. Limbachiya, M.S. Meddah, Y. Ouchagour, Use of recycled concrete aggregate in fly-ash concrete, Construction and Building Materials 27 (1) (2012) 439–449.
[130] W. Ling, T. Pei, Y. Yan, May. Application of ground granulated blast furnace slag in high-performance concrete in China, in: In *International Workshop on Sustainable development and Concrete Technology, organized by China building materials academy*, 2004, pp. 309–317.
[131] S. Liu, Z. Wang, X. Li, Long-term properties of concrete containing ground granulated blast furnace slag and steel slag, Magazine of concrete research 66 (21) (2014) 1095–1103.
[132] I. Löfgren, O. Esping, A. Lindvall, The influence of carbonation and age on salt frost scaling of concrete with mineral additions, Materials, Systems and Structures in Civil Engineering 2016 (2016) 91–100.
[133] G. Long, Y. Gao, Y. Xie, Designing more sustainable and greener self-compacting concrete, Construction and Building Materials 84 (2015) 301–306.

[134] W.J. Long, K.H. Khayat, A. Yahia, F. Xing, Rheological approach in proportioning and evaluating prestressed self-consolidating concrete, Cement and Concrete Composites 82 (2017) 105–116.
[135] A. Lübeck, A.L.G. Gastaldini, D.S. Barin, H.C. Siqueira, Compressive strength and electrical properties of concrete with white Portland cement and blast-furnace slag, Cement and Concrete Composites 34 (3) (2012) 392–399.
[136] S. Marinković, J. Dragaš, I. Ignjatović, N. Tošić, Environmental assessment of green concretes for structural use, Journal of Cleaner Production 154 (2017) 633–649.
[137] P.F. Marques, C. Chastre, Â. Nunes, Carbonation service life modelling of RC structures for concrete with Portland and blended cements, Cement and Concrete Composites 37 (2013) 171–184.
[138] V. Mary, C.H. Kishore, Experimental investigation on strength and durability characteristics of high performance concrete using ggbs and msand, ARPN Journal of Engineering and Applied Sciences 10 (11) (2015) 4852–4856.
[139] P.R. Matos, R.D. Sakata, L.R. Prudêncio Jr, Eco-efficient low binder high-performance self-compacting concretes, Construction and Building Materials 225 (2019) 941–955.
[140] M.J. McCarthy, R.K. Dhir, Development of high volume fly ash cements for use in concrete construction, Fuel 84 (11) (2005) 1423–1432.
[141] C. McNally, E. Sheils, Probability-based assessment of the durability characteristics of concretes manufactured using CEM II and GGBS binders, Construction and Building Materials 30 (2012) 22–29.
[142] A. Mittal, M.B. Kaisare, R. Shetti, Experimental Study on use of fly ash in concrete, Tarapur Atomic Power Project 3 (2005).
[143] E.G. Moffatt, M.D. Thomas, A. Fahim, Performance of high-volume fly ash concrete in marine environment, Cement and Concrete Research 102 (2017) 127–135.
[144] J. Mohammadi, W. South, Life cycle assessment (LCA) of benchmark concrete products in Australia, The International Journal of Life Cycle Assessment 22 (10) (2017) 1588–1608.
[145] Y. Murad, R. Imam, H.A. Hajar, A. Hammad, Z. Shawash, Predictive compressive strength models for green concrete, International Journal of Structural Integrity (2019).
[146] I.J. Navarro, V. Yepes, J.V. Martí, Life cycle cost assessment of preventive strategies applied to prestressed concrete bridges exposed to chlorides, Sustainability 10 (3) (2018) 845.
[147] M.C. Nepomuceno, L.A. Pereira-de-Oliveira, S.M.R. Lopes, Methodology for the mix design of self-compacting concrete using different mineral additions in binary blends of powders, Construction and Building Materials 64 (2014) 82–94.
[148] M.D. Newlands, M.R. Jones, M. McCarthy, L. Zheng, Using fly ash to achieve low embodied CO2 concrete. In *Proceedings of EUROCOALASH 2012 Conference*, 2012.
[149] T. Nochaiya, W. Wongkeo, A. Chaipanich, Utilization of fly ash with silica fume and properties of Portland cement–fly ash–silica fume concrete, Fuel 89 (3) (2010) 768–774.
[150] A. Oner, S. Akyuz, An experimental study on optimum usage of GGBS for the compressive strength of concrete, Cement and concrete composites 29 (6) (2007) 505–514.
[151] A. Oner, S. Akyuz, R. Yildiz, An experimental study on strength development of concrete containing fly ash and optimum usage of fly ash in concrete, Cement and Concrete Research 35 (6) (2005) 1165–1171.
[152] J. Park, S. Tae, T. Kim, Life cycle CO2 assessment of concrete by compressive strength on construction site in Korea, Renewable and Sustainable Energy Reviews 16 (5) (2012) 2940–2946.
[153] M.E. Parron-Rubio, F. Perez-Garcia, A. Gonzalez-Herrera, M.J. Oliveira, M. D. Rubio-Cintas, Slag substitution as a cementing material in concrete: Mechanical, physical and environmental properties, Materials 12 (18) (2019) 2845.
[154] Y.O. Patil, P.N. Patil, A.K. Dwivedi, GGBS as partial replacement of OPC in cement concrete–An experimental study, International Journal of Scientific Research 2 (11) (2013) 189–191.
[155] S.C. Kou, C.S. Poon, Long-term mechanical and durability properties of recycled aggregate concrete prepared with the incorporation of fly ash, Cement and Concrete Composites 37 (2013) 12–19.
[156] M.P. Preez, Sensitivity of strength and durability properties of blended cement concrete to changes in water/binder ratio and binder content, University of the Witwatersrand, Johannesburg, 2019. Doctoral dissertation.
[157] Quan, H.Z. and Kasami, H., 2014. Experimental study on durability improvement of fly ash concrete with durability improving admixture. *The Scientific World Journal*, *2014*.
[158] Rathnarajan, S., Vaddey, N.P., Pillai, R.G., Gettu, R. and Santhanam, M. 2017. Modelling carbonation rates in concretes with similar strength and with and without slag. *Conference: ICACMS 2017. Chennai,India*.
[159] E. Roziere, A. Loukili, F. Cussigh, A performance based approach for durability of concrete exposed to carbonation, Construction and Building Materials 23 (1) (2009) 190–199.
[160] H. Ruixia, A study on carbonation for low calcium fly ash concrete under different temperature and relative humidity, The Electronic Journal of Geotechnical Engineering (EJGE) 15 (2010) 1871–1877.
[161] D.W. Ryu, W.J. Kim, W.H. Yang, J.H. You, J.W. Ko, An experimental study on the freezing-thawing and chloride resistance of concrete using high volumes of GGBS, Journal of the Korea Institute of Building Construction 12 (3) (2012) 315–322.
[162] P. Saha, P. Debnath, P. Thomas, Prediction of fresh and hardened properties of self-compacting concrete using support vector regression approach, Neural Computing and Applications (2019) 1–16.
[163] M. Şahmaran, İ.Ö. Yaman, M. Tokyay, Transport and mechanical properties of self consolidating concrete with high volume fly ash, Cement and concrete composites 31 (2) (2009) 99–106.
[164] S. Samad, A. Shah, M.C. Limbachiya, Strength development characteristics of concrete produced with blended cement using ground granulated blast furnace slag (GGBS) under various curing conditions, Sādhanā 42 (7) (2017) 1203–1213.
[165] R. San Nicolas, M. Cyr, G. Escadeillas, Performance-based approach to durability of concrete containing flash-calcined metakaolin as cement replacement, Construction and Building Materials 55 (2014) 313–322.
[166] M.A. Sanjuan, C. Andrade, M. Cheyrezy, Concrete carbonation tests in natural and accelerated conditions, Advances in Cement Research 15 (4) (2003) 171–180.
[167] F.U. Shaikh, S.W. Supit, Compressive strength and durability properties of high volume fly ash (HVFA) concretes containing ultrafine fly ash (UFFA), Construction and building materials 82 (2015) 192–205.
[168] R. Siddique, Performance characteristics of high-volume Class F fly ash concrete, Cement and Concrete Research 34 (3) (2004) 487–493.
[169] M.G. Silva, M.R.M. Saade, V. Gomes, Influence of service life, strength and cement type on life cycle environmental performance of concrete, Revista IBRACON de Estruturas e Materiais 6 (6) (2013) 844–853.
[170] T. Simčič, S. Pejovnik, G. De Schutter, V.B. Bosiljkov, Chloride ion penetration into fly ash modified concrete during wetting–drying cycles, Construction and Building Materials 93 (2015) 1216–1223.
[171] K. Sisomphon, L. Franke, Carbonation rates of concretes containing high volume of pozzolanic materials, Cement and Concrete Research 37 (12) (2007) 1647–1653.
[172] Soja, W., 2019. *Carbonation of low carbon binders*. PhD Thesis. EPFL.Switzerland.
[173] Sonebi, M. & O'Donughue, V. & Keogh, G..2008. Effect of the Type of Supplementary Materials and Viscosity Enhancing Admixture on the Durability of Self-Compacting Concrete. *Proceedings of 11th International conf. on Durability of Building Materials and Components.* Istanbul.
[174] M. Soutsos, F. Kanavaris, A. Hatzitheodorou, Critical analysis of strength estimates from maturity functions, Case Studies in Construction Materials 9 (2018) e00183.
[175] Sugi, H., Tsukagoshi, M. and Ueda, T., 2013. Durability of concrete composites containing fly ash and blast furnace slag for use in for precast concrete products. In *Proceedings of 3rd International Conference on Sustainable Construction Materials and Technology, Kyoto, Japan.*
[176] S. Sujjavanich, P. Suwanvitaya, D. Chaysuwan, G. Heness, Synergistic effect of metakaolin and fly ash on properties of concrete, Construction and building materials 155 (2017) 830–837.
[177] S. Tae, C. Baek, S. Shin, Life cycle CO2 evaluation on reinforced concrete structures with high-strength concrete, Environmental Impact Assessment Review 31 (3) (2011) 253–260.
[178] S. Tsivilis, J. Tsantilas, G. Kakali, E. Chaniotakis, A. Sakellariou, The permeability of Portland limestone cement concrete, Cement and concrete research 33 (9) (2003) 1465–1471.
[179] G. Turu'allo, *Early age strength development of ggbs concrete cured under different temperatures* (Doctoral dissertation, University of Liverpool), 2013.
[180] M. Uysal, M. Sumer, Performance of self-compacting concrete containing different mineral admixtures, Construction and Building materials 25 (11) (2011) 4112–4120.
[181] P. Van den Heede, N. De Belie, Durability related functional units for life cycle assessment of high-volume fly ash concrete, Milwaukee, WI, USA, UWM Center for By-Products Utilization, 2010, pp. 583–594.
[182] E. Vejmelková, M. Pavlíková, Z. Keršner, P. Rovnaníková, M. Ondráček, M. Sedlmajer, R. Černý, High performance concrete containing lower slag amount: a complex view of mechanical and durability properties, Construction and Building Materials 23 (6) (2009) 2237–2245.
[183] E. Vejmelková, M. Keppert, S. Grzeszczyk, B. Skaliński, R. Černý, Properties of self-compacting concrete mixtures containing metakaolin and blast furnace slag, Construction and Building Materials 25 (3) (2011) 1325–1331.
[184] S.S. Vivek, G. Dhinakaran, Durability characteristics of binary blend high strength SCC, Construction and Building Materials 146 (2017) 1–8.
[185] A. Vollpracht, M. Soutsos, F. Kanavaris, Strength development of GGBS and fly ash concretes and applicability of fib model code's maturity function–a critical review, Construction and Building Materials 162 (2018) 830–846.
[186] D.D. Vu, P. Stroeven, V.B. Bui, Strength and durability aspects of calcined kaolin-blended Portland cement mortar and concrete, Cement and Concrete Composites 23 (6) (2001) 471–478.
[187] D. Wałach, P. Dybeł, J. Sagan, M. Gicala, Environmental performance of ordinary and new generation concrete structures—a comparative analysis, Environmental Science and Pollution Research 26 (4) (2019) 3980–3990.
[188] X.Y. Wang, Impact of Climate Change on the Optimization of Mixture Design of Low-CO2 Concrete Containing Fly Ash and Slag, Sustainability 11 (12) (2019) 3394.
[189] P. Woyciechowski, P. Woliński, G. Adamczewski, Prediction of carbonation progress in concrete containing calcareous fly ash co-binder, Materials 12 (17) (2019) 2665.
[190] G.Q. Xu, J.H. Liu, L. Qiao, Y.M. Sun, in: March. Experimental study on carbonation and steel corrosion of high volume fly ash concrete, IEEE, 2010, pp. 1–4.
[191] H. Yazıcı, The effect of silica fume and high-volume Class C fly ash on mechanical properties, chloride penetration and freeze–thaw resistance of self-compacting concrete, Construction and building Materials 22 (4) (2008) 456–462.

[192] K.Y. Yeau, E.K. Kim, An experimental study on corrosion resistance of concrete with ground granulate blast-furnace slag, Cement and Concrete Research 35 (7) (2005) 1391–1399.
[193] S.W. Yoo, G.S. Ryu, J.F. Choo, Evaluation of the effects of high-volume fly ash on the flexural behavior of reinforced concrete beams, Construction and building materials 93 (2015) 1132–1144.
[194] A. Younsi, P. Turcry, E. Rozière, A. Aît-Mokhtar, A. Loukili, Performance-based design and carbonation of concrete with high fly ash content, Cement and Concrete Composites 33 (10) (2011) 993–1000.
[195] A. Younsi, P. Turcry, A. Aït-Mokhtar, S. Staquet, Accelerated carbonation of concrete with high content of mineral additions: effect of interactions between hydration and drying, Cement and concrete research 43 (2013) 25–33.
[196] X. Zhang, X. Zhou, H. Zhou, K. Gao, Z. Wang, Studies on forecasting of carbonation depth of slag high performance concrete considering gas permeability, Applied Clay Science 79 (2013) 36–40.
[197] H. Zhao, W. Sun, X. Wu, B. Gao, The properties of the self-compacting concrete with fly ash and ground granulated blast furnace slag mineral admixtures, Journal of Cleaner Production 95 (2015) 66–74.
[198] N. Friedman, M. Linial, I. Nachman, D. Pe'er, Using Bayesian networks to analyze expression data, Journal of computational biology 7 (3–4) (2000) 601–620.
[199] https://bcc-regression.online/login/?next=/predict/.